Intracellular Responses of Glial Cells To Monomeric Tau Protein Are Closely Mediated By Heparan Sulfate Proteoglycans (HSPGs)

Liqing Song
Carnegie Mellon University
Daniel E. Oseid
Tulane University School of Science and Engineering
Evan A. Wells
Carnegie Mellon University
Troy Coaston
Tulane University School of Science and Engineering
Anne S Robinson (anne.robinson@cmu.edu)
Carnegie Mellon University College of Engineering https://orcid.org/0000-0001-7235-1481

Research Article

Keywords: Heparan sulfate, endocytosis, tauopathies, Alzheimer's disease, 0N4R tau, lipoprotein receptor

Posted Date: July 19th, 2021

DOI: https://doi.org/10.21203/rs.3.rs-647000/v1

Intracellular responses of glial cells to monomeric tau protein are closely mediated by heparan sulfate proteoglycans (HSPGs)

Liqing Song[1,a], Daniel E. Oseid[2, a], Evan A. Wells[1], Troy Coaston[2], and Anne S. Robinson[1,2]

1. Department of Chemical Engineering, Carnegie Mellon University, Pittsburgh, PA, 15213, USA

2. Tulane Brain Institute, Tulane University, New Orleans LA, 70118, USA

a. These authors contributed equally to this work.

*corresponding author: Anne S. Robinson, asrobins@andrew.cmu.edu; https://orcid.org/0000-0001-7235-1481

Abstract

The conversion of soluble tau protein to insoluble, hyperphosphorylated neurofibrillary tangles is a major hallmark leading to neuronal death observed in neurodegenerative tauopathies. Recent work suggests that extracellular, soluble tau binds to negatively charged heparan sulfate proteoglycans (HSPGs) available on the cell surface. In addition, LRP1 has recently been recognized as a major tau receptor, mediating tau uptake and spread. We hypothesized based on this data that monomeric tau would be endocytosed in both an HSPG- and LRP-dependent manner, activating intracellular signaling pathways that would regulate cellular phenotypes. Using live-cell confocal microscopy and flow cytometry, we show that soluble 0N4R monomers were rapidly endocytosed by SH-SY5Y and C6 glioma cells, via actin-dependent macropinocytosis. We also demonstrated the crucial role of HSPGs and LRP1 in cellular endocytosis of monomeric tau by observing reduced tau uptake in C6 glial cells with genetic knockouts of xylosyltransferase-1 – a key enzyme in HSPG synthesis – and LRP1. An ERK1/2 inhibition experiment showed that inhibiting the MEK-ERK1/2 signaling pathway attenuated *IL-6* and *IL-1β* gene expression but not *TNF-α*. An *LRP1* knockdown experiment led to an attenuated propensity for tau uptake and further elevated *IL-6* gene expression. Collectively, our data suggest that tau has multiple extracellular binding partners that mediate its internalization through distinct mechanisms. Additionally, this study demonstrates the important role of both HSPG and LRP1 in regulating cellular immune responses to tau protein monomer, which provides a novel target for alleviating the neuroinflammatory environment before the formation of neurofibrillary tangles.

Keywords: Heparan sulfate, endocytosis, tauopathies, Alzheimer's disease, 0N4R tau, lipoprotein receptor

Abbreviations: AD, Alzheimer's disease; HSPG, heparan sulfate proteoglycans; NFT, neurofibrillary tangles; Xylt1, xylosyltransferase-1; FTD, frontotemporal dementia; CNS, central nervous system; Aβ, β-amyloid peptide; ISF, interstitial fluid; CSF, cerebrospinal fluid; HSPG, Heparan sulfate proteoglycans; HS, heparan sulfate; LRP1, Low-density lipoprotein receptor-related protein 1; MT, microtubules

Declarations

Funding: This research was supported in part by the Marko Spark Innovation fund (Tulane University Brain Institute) and by Carnegie Mellon University.

Conflicts of interest/Competing interests: Nothing to declare

Availability of data and material (data transparency): The datasets generated during and/or analyzed during the current study are available from the corresponding author on reasonable request.

Code availability: Nothing to declare.

Authors' contributions: All authors contributed to the overall study conception and design and Anne S. Robinson was responsible for overall supervision. Material preparation, data collection and analysis were performed by Liqing Song, Daniel E. Oseid, Evan A. Wells. The first draft of the manuscript was written by Liqing Song and all authors commented on previous versions of the manuscript. All authors read and approved the final manuscript.

Additional declarations for articles in life science journals that report the results of studies involving humans and/or animals: Nothing to declare.

The authors thank Dr. Deborah Grimm (Tulane University) for assistance with confocal microscopy experiments and analysis.

Introduction

More than twenty-five neurological disorders feature filamentous aggregates of hyperphosphorylated tau protein in the brain and are collectively known as neurodegenerative tauopathies [1]. Progressive deposition of tau-containing neurofibrillary tangles (NFTs) throughout various brain regions is a well-characterized hallmark of tauopathies; however, the mechanism behind NFT formation and spread remains poorly understood. Tau binds and stabilizes axonal microtubules (MTs) but can be hyperphosphorylated and lose its affinity for MTs [2]. MAPT gene mutation has also been proposed to explain the impaired ability of tau to promote the assembly of tau and MTs [3], leaving it available to interact with other cellular components. Indeed, in the past few decades many additional binding partners, subcellular locations, and physiological roles of tau have been identified [4].

Increasing evidence suggests that tau can be physiologically released into the extracellular space, both as monomers and aggregate forms. Tau has been found in both the interstitial fluid (ISF) and cerebrospinal fluid (CSF) in both humans and wild-type rodents, suggesting that tau release can occur in the absence of neurodegeneration [5][6][7][8][9][10]. Many species of tau have been characterized outside of cells including free monomer, C-terminal truncations, low molecular weight aggregates, fibrils, or membrane-encapsulated tau [11][12][13][14]. Interestingly, endogenous tau was released in an activity-dependent manner from primary cortical cultures [15]. Several cell culture studies show that tau monomer and oligomer in various phosphorylation states are constitutively released into the extracellular space [12][16][17]. Tau monomer in the ISF may eventually have pathogenic consequences as tau monomers are able to adopt both an inert and a seed-competent conformation, while some seed-competent monomers can form multiple unique pathological strains [18][19]. Furthermore, full-length, soluble tau monomer added externally to culture media eventually forms aggregates inside cells [20]. Taken together, these findings suggest that cellular uptake of physiologically released tau monomer may represent an initial step in neurodegenerative tauopathies, where cellular uptake provides the initial conditions for aggregation.

Several groups have demonstrated that full-length monomer is readily internalized through clathrin-mediated endocytosis or macropinocytosis and that this internalization depends on heparan sulfate proteoglycans (HSPGs) [21][22]. In contrast, some studies have shown that only low molecular weight tau trimers or larger are endocytosed while monomer is not [23][24][25][26]. HSPGs are emerging as a likely mediator of tau internalization as tau contains several heparin-binding domains [27]. However, a member of the low-density lipoprotein receptor family, LRP1, also had a significant effect on tau endocytosis by neuronal cells [27].

Cellular responses following monomeric tau uptake have yet to be widely reported in the field of neurodegeneration research. Phosphorylation or mutation may affect the conformation of wild-type tau

protein and could have increased pathogenic consequences on the cell by converting wild-type tau into a more pathological relevant tau protein seed, leading to the subsequent pathological transmission, as discussed in one of our previous papers [28]. This possibility also merits further investigation. Recently, the involvement of astrocytes in the progression of tau pathology has drawn much attention because of their close communication with neuronal cells [28][29][30]. Astrocytes, like microglia, express genes involved in phagocytosis [31], eliminate synaptic debris [32], or protein aggregates as seen by clearance of β-amyloid peptide (Aβ) [33]. For instance, the enhanced cellular uptake of tau fibrils by astrocytes has been related to the intensive autophagy-lysosomal pathway as reported in several tau pathology mouse models. Moreover, astrocytes develop more neurotoxic features by transforming into reactive astrocytes, which are induced by activated microglia and neuroinflammation in various human neurodegenerative disorders at a more advanced stage [34]. However, the cellular responses of astroglial cells to tau monomers have been less investigated. Most importantly, astrocytic LRP1 has been implicated in Aβ cleavage during the progression of Alzheimer's Disease (AD), while the mechanism by which LRP1 regulates cellular uptake of tau monomers in glial cells requires further investigation.

In this study, cellular endocytosis of tau monomer was examined in several cell lines, as well as neuronal and glial cells. To investigate the molecular contributors to tau endocytosis and altered intracellular activities, we subsequently examined tau uptake propensity and the resulting cellular signaling pathways in HSPG and LRP1-deficient glial cells. Findings from this study provide novel information for the progression of tau protein-related pathology and shed light on exacerbated pro-inflammatory signaling pathways affected by tau propagation that may provide a therapeutic target.

Materials and Methods

Recombinant Protein Expression and Purification

Full-length tau (0N4R isoform described in Morozova et. al [35]) was subcloned into pETM-13 (https://www.embl.de/pepcore/pepcore_services/strains_vectors/vectors/bacterial_expression_vectors/), and GSK-3β (a gift of the Woodgett lab, RRID:Addgene_15898) was subcloned into pBAD (EMBL). Both plasmids were generated using ligation-independent cloning [36]. A triple tau mutant (VPR) containing P243L, V279M, and V348W in the wild-type 0N4R tau isoform was created using site-directed mutagenesis (GeneArt® Site-Directed Mutagenesis System, ThermoFisher Scientific). P243L, V279M, and V348W in 0N4R correspond to the P301L, V337M, and R406W positions in the full-length 2N4R. The oligonucleotide sequences were as follows: P243L (CCG->CTG): 5'-GATAATATCAAACACGTCCTGGGAGGCGGCAGTG-3', V279M (GTG->ATG): 5'-

CAGGAGGTGGCCAGATGGAAGTAAAATCTGAG-3', and V348W (CGG->TGG): 5'-GACACGTCTCCATGGCATCTCAGCAATGTCTCC-3'. The pETM-13-0N4R tau plasmid was transformed by heat-shock into chemically competent Rosetta™(DE3) cells (MilliporeSigma, 70954) using standard techniques [37], and selected with 34 µg/mL chloramphenicol and 50 µg/mL kanamycin, with 100 µg/mL ampicillin added for pBAD-GSK3β plasmid selection. Positive clones containing 0N4R tau were grown in LB media containing 34 µg/mL chloramphenicol and 50 µg/mL kanamycin, and if expressing phospho-tau with 100 µg/mL ampicillin to maintain the GSK-3β plasmid. For protein production, cells were inoculated and grown in Terrific Broth (24 g/L Yeast extract, 20 g/L tryptone, 4 mL/L glycerol) at 37 °C until the A600 was between 0.5 and 0.9. To induce tau expression, isopropyl β-D-1-thiogalactopyranoside (IPTG) was added to a final concentration of 0.5 mM, and the culture was grown for 4 hours at 37 °C. For phospho-tau expression, the cells co-transformed with pETM-13-0N4R and pBAD-GSK3β also received arabinose at a final concentration of 0.1%, added at the same time as the IPTG. The bacterial cells were pelleted by centrifugation at 10,000 x g and tau directly purified, or the pellet frozen at -80 °C prior to purification.

Tau proteins were purified as described previously [38]. Briefly, pelleted cells were resuspended in a high-salt buffer (0.1 M MES, 1 mM EGTA, 0.5 mM MgSO4, 0.75 M NaCl, 0.02 M NaF, 1 mM PMSF, pH 7.0), disrupted via sonication, and centrifuged at 3200 x g to remove insoluble debris. The supernatant was decanted and then boiled for 10 minutes, cooled on ice for 15 minutes, and then centrifuged at 3200 x g for 10 minutes to remove and discard precipitated protein. The supernatant was decanted and dialyzed overnight at 4 °C in column wash buffer (20 mM PIPES, 10 mM NaCl, 1 mM EGTA, 1 mM $MgSO_4$, 2 mM DTT, 0.1 mM PMSF, pH 6.5). The dialyzed lysate was applied to an SP-sepharose cation-exchange column on a BioLogic DuoFlow chromatography system (Bio-Rad); following application, the column was washed for 10 column volumes and protein eluted with 0.4 M NaCl. Protein-containing fractions were combined, buffer-exchanged into PBS, and concentrated using Amicon® Pro purification concentrators (10 kDa MWCO, ACS501002, MilliporeSigma). The protein concentration was determined from measuring the absorbance at 280 nm (A280) using Beer's Law with $\epsilon = 7450\ M^{-1}\ cm^{-1}$ and MW= 40 kDa. A typical final yield was 10-12 mg of tau per liter of culture.

Cell Culture

SH-SY5Y neuroblastoma cells (ATCC CRL-2266™; RRID:CVCL_0019) were cultured in a 1:1 mixture of HAMS and Minimal Essential Media, containing 10% fetal bovine serum (FBS). C6 glioma cells (ATCC CCL-107™; RRID:CVCL_0194) were cultured in HAMS and 15% horse serum (ATCC) and 2.5% FBS. HEK293 cells (ATCC CRL-1573™; RRID:CVCL_0045) were cultured in DMEM and 10%

FBS. CHO745 cells and CHO cells (ATCC CRL-9618™; RRID:CVCL_0214) were cultured in 10% FBS and HAMS (ATCC). Rat primary astrocytes (iXCells Biotechnologies 10RA-005) were cultured in astrocyte medium (Thermo Fisher Scientific, USA), 2% FBS and 100 U/ml Penicillin-Streptomycin. Cell cultures were maintained in a humidified atmosphere of 5 % CO_2 at 37 °C and cultured in CELLSTAR 25 cm^2 culture flasks with filters.

CRISPR Plasmid Design and Construction

Primers of single guide RNAs (sgRNAs) were designed with Benchling online CRISPR Guide RNA Design Tool (https://www.benchling.com/crispr/) that designs sgRNAs with input target sites and provides on- and off-target scores for optimizing higher activity and lowering off-target effects. sgRNAs were designed to target the xylosyltransferase domain; the Exon7-targeting sequence (CCTGTATGGCAACTATCCTG) on the *Xylt1* gene (Acc:620093) was introduced into the pSpCas9(BB)-2A-GFP (RRID:Addgene_48138, a gift of Feng Zhang) using established cloning protocols with BbsI and T7 ligase. The ligation reaction was transformed into *E. coli DH5α* and the sgRNA expression plasmid obtained via selection of colonies on ampicillin-containing LB plates. Sequences were confirmed using the U6 promoter forward primer: GAGGGCCTATTTCCCATGATT (Integrated DNA Technologies, USA).

C6 Transfection

Twenty-four hours before transfection, C6 cells were seeded at 7×10^5 cells per well in a 6-well plate containing 2 mL of complete growth medium. Cells were grown overnight to approximately 80-90% confluency. On the day of transfection, cells were harvested with 0.05% Trypsin- EDTA and transfected with the sequence-confirmed sgRNA plasmid constructs. For optimizing transfection conditions, 1×10^6 C6 cells were transfected with 10 µg DNA using the SF Cell line 4D-Nucleofector™X kit (V4XC-2012, Lonza) according to the manufacturer's specifications. Cells were incubated in a humidified 37 °C, 5 % CO_2 incubator for 48 hrs.

Fluorescence-Activated Cell Sorting (FACS) of Transfected Cells for Nuclease-expressing Cells

Two days post-transfection, C6 cell samples were detached with 0.05% Trypsin- EDTA and the top 3% of GFP positive cells were sorted by FACS into prepared 1.5 ml Eppendorf tubes to enrich the cell population with higher levels of nuclease expression. Following a one-week expansion, enriched cell populations were subjected to a second round of transfection with the sgRNA expression plasmid to

improve the level of genome editing, by following the same procedure. Two days post-transfection, transfected cells were harvested and sorted individually into 96-well plates, followed by a two-week expansion in a humidified incubator. The single cell clone (CL5) used for experimentation was selected by indel detection by amplicon analysis (IDAA) DNA capillary electrophoresis [39].

Alexa Fluor Labeling

Different isoforms of tau protein were labeled with either Alexa Fluor™ 488 (AF488) NHS Ester or Alexa Fluor™ 647 (AF647) NHS Ester (Life Technologies, USA) according to the manufacturer's instruction by incubating the label and protein (1:10 w/w) in sodium bicarbonate (pH 8.3) for 1 hour at room temperature. A Sephadex G-25 column (GE Healthcare) was used to separate labeled protein from the free label and the recovered labeled protein – referred to as tau-488 or tau-647 – was concentrated using Amicon® Pro purification concentrators (10 kDa MWCO) and quantified via A280 measurement prior to the use.

Live Cell Confocal Microscopy

All cells were plated at 50,000 cells/well in Lab-Tek II confocal imaging chambers (Thermo-Fisher, cat# 155360) and cultured for 24-48 hours in incubators prior to assay. On the day of assay, cell chambers were transferred to a pre-warmed live-cell imaging chamber slide incubator on a Nikon A1 confocal microscope and allowed to equilibrate for approximately 10 min. at 37 °C and 5 % CO_2. All data acquisition was performed with a 488 nM excitation laser with a 60x oil-objective attached to a heating element to prevent heat-sink from the imaging chamber during acquisition. Thirty seconds after acquisition began, a pre-warmed protein-media mixture was added to cells in a 2X concentration to ensure complete mixing. For analysis, each cell was monitored to determine the number of tau-containing vesicles – where fluorescent signals appeared as distinct puncta in the cytoplasm – as a function of time. Three independent biological replicates were performed for all cells and at least three cells per sample were analyzed. To block non-specific endocytosis, cells were pre-incubated on loosely packed wet ice for 30 min. For experiments blocking macropinocytosis via chemical means, culture media was replaced fully with either 1.0 or 0.1 μM cytochalasin-D (MilliporeSigma C8273) for 30 min. prior to tau addition to cells.

Tau Internalization Assay and Flow cytometry

To test the tau uptake propensity by different cell types (HEK293, SH-SY5Y, C6 glioma), single-cell C6 subclone (CL5), *LRP1* knockdown C6 cells, and primary rat astrocytes (RA) were seeded at 5×10^5 cells/well in a 24-well plate. After culturing overnight, cells were incubated with tau-AF488 at fixed incremental concentrations of tau proteins (0.25 μM, 0.5 μM, and 1.0 μM). After at least 30 mins., the cells were washed with PBS, trypsinized with 0.05% Trypsin-EDTA (Thermo Fisher Scientific, USA), and the fluorescence analyzed with an Accuri flow cytometer (MBIC, Mellon Institute). The relative tau uptake for each condition was calculated by subtracting the non-specific binding of the fluorophore to the cell membrane, which was conducted with identical experimental procedures but at 4 ℃ to limit internalization. For some experiments, C6 glioma, CL5, or primary rat astrocytes (RA) were incubated with unlabeled tau proteins – wild-type 0N4R (tau), phospho-0N4R (ptau) and a triple 0N4R mutant (VPR) – at 1 μM for 48 hrs. before characterization by Western Blotting and quantitative real-time PCR analysis. For experiments to investigate the effects of heparin on tau uptake by cells, 0.5 mg/ml heparin (Amsbio, AMS.HEP001) along with the tau protein was added to cell culture, as indicated.

Western Blotting

For analysis of tau present in mammalian cells, the cells were trypsinized and washed with ice-cold PBS prior to suspension in RIPA lysis buffer containing 150 mM NaCl, 0.1 % (v/v) Triton X-100, 0.5 % (w/v) sodium deoxycholate, 0.1 % (w/v) SDS, 50 mM Tri-HCL, and Halt™ Protease and Phosphatase Inhibitor Cocktail (Thermo Fisher Scientific, USA) for protein extraction. The cell lysate was maintained at constant agitation for 30 min. at 4 °C followed by centrifugation at 16,000 x g for 20 min. at 4 °C. Protein concentration was determined by BCA assay (Thermo Fisher Scientific, USA). Prior to gel electrophoresis, cell lysate was mixed with a 4X Laemmli sample loading buffer (Bio-Rad, USA) and boiled at 95 °C for five min. Equal amounts of cell lysate were loaded into the wells of a Mini-PROTEAN TGX Precast Gel (Bio-Rad, USA), along with Precision Plus Protein™ WesternC™ standards (Bio-Rad, USA) and then electrophoresed for 30 min. at 225 V. Proteins were then transferred to 0.2 μm preassembled PVDF membrane (Bio-Rad, USA) using the Trans-Blot Turbo Transfer System (Bio-Rad, USA). The blots were then subjected to Western analysis as described previously [40]. Briefly, blots were incubated with 5 % nonfat dried milk in 1X Tris-buffered saline containing 0.1 % (v/v) Tween-20 (TBS-T) buffer for 1 hr. at room temperature to block non-specific binding, and incubated with the primary antibodies phospho-ERK1/2 (Cell Signaling, 9101S), ERK1/2 (Cell Signaling, 9102S), Xylt1 (Life Technologies, PA5-67627), and endogenous control protein, β-actin (Cell Signaling, 3700T), in TBS-T containing 5 % (w/v) BSA

overnight at 4 °C. After washing with 1X TBS-T, the blot was incubated with the fluorophore-conjugated secondary antibody (Li-Cor Biosciences, 926-32211) for 1 hr. at room temperature. The blots were imaged with ChemiDoc MP Imaging System (Bio-Rad, USA) and the band intensities of target proteins were normalized to the endogenous control protein, β-actin, using ImageJ software.

Quantitative Real-time PCR Analysis

Total RNA was isolated from cell samples using the RNeasy Plus Mini Kit (Qiagen) according to the manufacturer's protocol, followed by treatment with the RNA Clean & Concentrator Kit (Zymo). Reverse transcription of 2 μg of total RNA was carried out using the High-Capacity cDNA Reverse Transcription Kit (Applied Biosystems) according to the protocol of the manufacturer. Primers used in the real-time PCR are listed in **Supplementary Table 1**. The gene β-actin was used as an endogenous control for the normalization of expression levels. Real-time PCR reactions were performed on a ViiA™ 7 System using PowerUp™ SYBR™ Green Master Mix (Applied Biosystems). The amplification reactions were performed as follows: 15 min. at 50 °C, 10 min. at 95 °C, and 40 cycles of 95 °C for 15 s and 60 °C for one min. Fold-change in gene expression was quantified by means of the comparative Ct method, which is based on the comparison of the target gene expression (normalized to the endogenous control β-actin) between the samples. For experiments designed to inhibit MEK1/2-ERK1/2 signaling, 100 μM MEK1/2-ERK1/2 inhibitor, U0126-EtOH (Selleckchem, S1102), was added to culture media along with tau protein.

Immunocytochemistry

Cell staining was performed as described previously [41]. Briefly, 1×10^6 cells per sample were fixed with 4 % (w/v) paraformaldehyde in PBS and washed with a staining buffer (2 % (v/v) FBS in PBS). For staining intracellular markers, the samples were permeabilized with 0.2 – 0.5 % (v/v) Triton X-100. The cells were then blocked with 10 % (v/v) FBS and incubated with primary antibodies, mouse anti-Heparan Sulfate (HS; USBiologic, H1890), or mouse anti-Glial Fibrillary Acidic Protein (GFAP, Sigma-Aldrich, MAB360-25UL) for 4 h. After washing, the cells were incubated with the corresponding secondary antibody: Alexa Fluor® 488 goat anti-Mouse IgM (Abcam, ab150121) and Alexa Fluor® 488 goat anti-Mouse IgG1 (Life Technologies, A21125), for 1 h. The samples were counterstained with Hoechst 33342 (Abcam, ab228551) and visualized using a fluorescent microscope (Keyence BZ-X810).

LRP1 Knockdown by Small Interfering RNA (siRNA)

Double-stranded, rat *LRP1* specific siRNAs and non-targeting siRNA were synthesized by IDT. The sequences of *LRP1* specific siRNAs were as follows:
LRP1 siRNA1: 5'- GGCGUCACUUACAUCAACAACCGTG-3',
LRP1 siRNA2: 5'- CCUGAUGUUCUGGACCAAUUGGAAT-3', and
LRP1 siRNA3: 5'- GUAAAAAUGAAGGAAUUACUUUUTA-3'.
1×10^6 C6 glioma cells were transfected with *LRP1*-specific siRNAs (300nM) and non-targeting siRNA using Lonza's SF Cell line 4D-Nucleofector™X kit (V4XC-2012, Lonza) according to the manufacturer's specifications. Cells were incubated in a humidified 37 °C, 5 % CO2 incubator for 48 hrs. Gene expression of *LRP1* was analyzed by real-time PCR analysis 48 hrs. after transfection.

Statistical Analysis

Statistical significance was determined by unpaired t-tests, one-way analysis of variance (ANOVA), or two-way ANOVA when appropriate using GraphPad Prism 8 software. A five percent cutoff was applied to determine statistical significance, and a p-value of <0.05 was denoted with one asterisk (*). In all cases, at least three independent biological replicates from different days were performed and the standard error of the mean is shown.

Results

0N4R tau is rapidly endocytosed by immortalized cell lines via actin-dependent macropinocytosis pathway

We employed both live-cell confocal microscopy and flow cytometry to give insights into the kinetics of 0N4R tau endocytosis in three immortalized cell lines (**Fig. 1**). Purified 0N4R tau protein monomer was labeled with Alexa Fluor 488 dye (tau-488) as described in materials and methods, and quantification of live-cell confocal microscopy as number of vesicles per cell showed that rat C6 glioma cells endocytosed tau-488 monomer around three to four times as rapidly as HEK293 cells and SH-SY5Y cells (**Fig. 1A and 1B**). This result was corroborated by quantitative flow cytometry analysis, as 99% of C6 glioma cells were positive for tau after 15 min. compared with 75.2% for SH-SY5Y cells and just 6.8% for HEK293 cells for 1 μM tau addition (**Fig. 1C-E**). Importantly, free Alexa Fluor 488 label and bovine serum albumin (BSA; 1 μM) labeled with Alexa Fluor 488 did not enter cells over the imaging periods used (**Supplemental Fig. S1**), suggesting that bulk fluid-phase endocytosis was not responsible for the rapid uptake of 0N4R tau that was observed. Because tau probably exists in lower concentrations in the ISF as

compared with the cytosol in living systems [10], we also tested uptake of 25 nM tau-488 for all three cell types (**Fig. 1C-E**). We observed a decrease in tau-488 fluorescence in SH-SY5Y and HEK293 cells over the time periods tested; however, no statistically significant difference was observed in C6 glioma cells for the 25 nM versus the 1 μM tau addition (**Fig. 1E**).

To confirm that this process occurred via cellular endocytosis, we pre-incubated HEK293 cells on ice for thirty minutes prior to tau addition and found that tau-488 monomer did not enter cells at temperatures non-permissive for endocytosis, as determined by confocal microscopy (**Fig. 2A and 2B)**. Furthermore, flow cytometry confirmed that HEK293 cells preincubated at 4 °C endocytosed approximately seven times less tau-488 than cells incubated at 37 °C (**Fig. 2C**). To understand the molecular mechanism responsible for tau endocytosis, SH-SY5Y cells – an effective model of neurodegeneration [42] – were preincubated with cytochalasin-D as a potent actin-polymerization and macropinocytosis inhibitor. Cytochalasin-D addition reduced tau uptake significantly over the entire observation time (**Fig. 2D**). Tau pathology is not solely restricted to neuronal cells, as tau inclusions have been found in astrocytes, oligodendrocytes, and even microglia [43][44]; therefore, we also sought to validate a similar tau uptake mechanism in an immortalized glial cell line, the rat C6 glioma line. Diminished tau uptake was also observed in C6 glial cells (**Fig. 2D**) with the addition of cytochalasin-D. Taken together, these data suggest that 0N4R tau monomer is readily endocytosed by all three immortalized cell lines, largely by actin-mediated macropinocytosis.

C6 glioma cells efficiently endocytose 0N4R monomer in an HSPG-dependent manner

Because tau endocytosis in both monomeric and oligomeric states has previously been shown to depend on the presence of heparan sulfate proteoglycans (HSPGs) [26][45]. Heparin, a glycosaminoglycan, has been used to competitively inhibit binding of 2N4R tau to HSPGs, as well as other entities in the extracellular space such as viruses [46]. To relate tau endocytosis to HSPGs on the cell surface, tau uptake was examined in CHO and CHO745 – a CHO-derived cell line deficient in xylosyltransferase, thus incapable of synthesizing all glycosaminoglycans (GAGs) [47]. Quantitation of live-cell imaging showed that CHO745 cells rapidly endocytosed tau monomer but did so at a significantly slower rate than wild-type CHO cells (**Fig. 3A**). To further our understanding, heparan sulfate (HS) protein expression on the cell surface was quantified by immunolabeling and flow cytometry analysis (**Fig. 3B**). The relative expression levels are consistent with the differential endocytosis rate we observed (**Fig. 1**), where C6 cells had the highest expression of HS as well as the highest endocytosis rate across all the cell lines we tested, and as expected, CHO showed higher levels of HS relative to the CHO745, consistent with observed tau uptake.

To validate our hypothesis about the importance of HSPGs as key cell surface receptors for tau, we then constructed an HSPG-deficient C6 cell line by genetic knock-down of xylosyltransferase (*Xylt1*) using the clustered regularly interspaced short palindromic repeat (CRISPR)-Cas9 system [48]. This approach was informed by the previous approach in CHO cells that showed that Xylt1 deficiency would prevent glycosaminoglycan production and directly disrupt HSPG biosynthesis [47], Single guide RNA (sgRNA) was designed to target Exon7 of *Xylt1*, within the xylosyltransferase domain (**Fig. 4A**). C6 wild-type cells were transfected with a sequence-verified CRISPR/Cas9-sgRNA construct according to this design. We observed a higher level of GFP expression for transfected cells, while cells lacking the template showed no fluorescence (**Fig. 4B**). The top 3% of the GFP-positive cell population was subjected to FACS-based single-cell selection (see materials and methods), and two clones were characterized following fragment length analysis – clone 3 (CL3), and clone 5 (CL5). As Xylt1 catalyzes the first step in the biosynthesis of HSPG, the levels of heparan sulfate (HS) were quantified by immunostaining to validate the knockdown. Flow cytometry analysis of these stained populations showed that CL5 had about half the HS expression compared with the non-edited C6 parental cells, while CL3 showed a similar level of HS expression compared with the parental cells (**Fig. 4C**). To confirm the HS expression data, mRNA levels of *Xylt1* were quantified, with *Xylt1* gene expression of CL5 observed to be about two-fold lower than the non-edited parental C6 (**Fig. 4D**). Western blot analysis confirmed the absence of Xylt1 expression in CL5, compared with non-edited parental C6 (**Fig. 4E**). These data confirmed the successful creation of a *Xylt1*-knockdown C6 cell line that will be referred to as CL5, by using the CRISPR/Cas9 system, which was used for subsequent studies.

Uptake of tau-488 by CL5 was then compared with parental C6 cells (**Fig. 4F**). Tau-488 was rapidly and efficiently internalized by C6 cells in a concentration-dependent manner, while the HSPG deficiency in CL5 significantly decreased the cellular uptake of tau at every concentration measured during a thirty-minute incubation. These data indicate that HSPGs indeed play a significant role in the uptake of 0N4R tau monomers by glial cells.

Intracellular responses stimulated by tau internalization is HSPG-dependent

Stancu and colleagues [49] showed previously that aggregated tau was capable of activating the NLRP3 inflammasome, increasing secretion of proinflammatory cytokines. Uptake of fibrillar Aβ also induced the assembly of the NLRP3 inflammasome, which led to caspase 1-dependent release of pro-inflammatory cytokines such as IL-1β and IL-18 [50]. To identify the cellular events affected by tau monomer endocytosis in C6 glial cells, we next evaluated mRNA transcriptional levels of the pro-inflammatory cytokines, IL-6 and TNF-α. Wild type 0N4R tau addition significantly upregulated pro-

inflammatory gene expression of *IL-6* and *TNF-α* (**Fig. 5Ai**), suggesting a direct role in activating a pathological cascade in glial cells.

As previous studies demonstrated that the activation of the MEK/ERK pathway was associated with early tau deposition in neurons and glial cells in tauopathies [51], we recognized that ERK1/2 phosphorylation might lead to cytokine transcription. Internalization of Aβ during the progression of neurofibrillary degeneration in Alzheimer's Disease (AD) has also led to MEK/ERK pathway activation [52]. To explore the potential mechanism through which tau induced immune responses, the phosphorylation of ERK1/2 was further examined for different experimental conditions [53]. Intriguingly, the phosphorylation of ERK1/2 increased in glial cells following tau monomer addition as compared with control cells, as determined by Western analysis (**Fig. 5B**).

To further understand whether cytokine addition was affected by physiological tau differently from pathological tau, several tau variants were examined. A triple mutant VPR (V337M, P301L, R406W) associated with frontotemporal dementia (FTD) that has been shown to hyperphosphorylate and have increased aggregation propensity [54][55] and a highly phosphorylated tau protein (ptau) that is expected to drive aggregation [56] were created as described in materials and methods, and purified as for wild-type tau. Interestingly, the highest ERK1/2 phosphorylation was concurrent with the highest expression of immune genes in the C6 cells incubated with VPR or ptau (**Fig. 5Ai and 5B**). Addition of the MEK-ERK1/2 inhibitor U0126 abolished the increased levels of *IL-1β* and *IL-6* and enhanced *TNF-α* mRNA levels that were induced by exogenous VPR addition (**Fig. 5Aii**). Taken together, we conclude that tau monomer addition induced gene expression changes of pro-inflammatory cytokines, which are regulated by ERK1/2 activation.

HSPGs have been implicated in cellular signaling from a variety of ligands, such as the Wnt, Hedgehog, transforming growth factor-β, and fibroblast growth factor during development [57]. To investigate the relevance of HSPGs and intracellular signaling activation by tau addition, we further evaluated ERK1/2 phosphorylation and mRNA transcriptional levels of the proinflammatory cytokines IL-6 and TNF-α in the HSPG-deficient C6-derived cell clone CL5. Intriguingly, CL5 cells displayed minimal activation of pro-inflammatory genes upon tau monomer addition compared to parental C6 (**Fig. 5Aiii**) and the phosphorylation of ERK1/2 was decreased (**Fig. 5C**). These data suggest that HSPGs regulate the pro-inflammatory gene expression of glial cells in response to monomeric tau via ERK1/2 signaling activation.

Heparin attenuates tau uptake and mitigates immune response to tau in primary astrocytes

In order to ensure the observations were not limited to immortalized cell lines, experiments in primary astrocytes were performed to determine the effects of heparin in regulating intracellular activities affected by tau endocytosis. The propensity for tau uptake was examined in rat primary astrocytes by fluorescent imaging or flow cytometry to visualize and quantify tau internalization. Monomeric VPR-488 was rapidly internalized by the primary astrocyte (**Fig. 6A**), and the amount of internalized tau increased over time from 1 hr. to 6 hrs., while heparin addition attenuated the tau uptake, indicating tau uptake was partially mediated by HSPGs. Phase-contrast images were overlaid with fluorescent images to visualize the spatial localization of tau, where tau protein was observed to be localized primarily within the cell body (**Fig. 6A**). Additionally, the nuclear stain Hoechst and an astrocyte-specific marker, GFAP, were co-imaged with VPR-488 to determine the spatial distribution of tau relative to the cell nucleus (**Fig. 6B**). Tau protein was evenly distributed outside of the cell nucleus, with negligible overlap with intracellular GFAP protein. In order to quantify this observation, monomeric VPR-488 uptake was determined in primary astrocytes by flow cytometry (**Fig. 6C and D**), showing that all cells appear to take up tau following a 6-hour incubation. Heparin addition led to a 50% decrease in tau uptake compared to the control group without heparin addition. A similar effect of heparin reduction of wild-type tau and ptau internalized by astrocytes was observed (**Supplemental Fig. S2**), suggesting heparin competes with tau for binding with HSPGs at the cell surface, regardless of physiological tau state. Further, the presence of heparin also ameliorated the immune activation of astrocytes upon the addition of unlabeled monomeric VPR by driving the *IL-6* and *IL-1β* gene expression back to baseline levels, though TNFα levels remained elevated (**Fig. 6E**).

LRP1 receptor plays a role in regulating intracellular responses of glial cells to tau protein

LRP1 has been recently identified as a major regulator of tau internalization, and tau transmission in neurons [58]. Ligand binding to LRP1 also activates cytoplasmic signaling pathways including several important intracellular mediators such as JNK and ERK and has been shown to mediate the immune responses of microglia to extracellular signals [59]. To identify potential interactions between HSPGs and LRP1 upon tau addition, we measured *LRP1* expression in both C6 cells and CL5 cells. The addition of VPR protein downregulated *LRP1* levels in C6 cells while *LRP1* levels in CL5 cells remained at similar levels as the parental C6 cells (**Fig. 7A**). While the cellular mechanism underlying the interplay between HSPG and *LRP1* expression needs further investigation, these data clearly indicate that HSPG levels mediate *LRP1* expression in the presence of tau.

To validate our observation and identify the role of LRP1 in regulating intracellular responses to monomeric tau, *LRP1* gene expression was reduced in C6 glial cells using specific *LRP1*-siRNAs. *LRP1* was successfully knocked down by 20%-70% using three different *LRP1*-siRNA (**Fig. 7B**). *LRP1*-siRNA3 knockdown cells and control cells were incubated with 1 μM VPR-488 at 37 °C for 30 minutes and then analyzed by fluorescent microscopy (**Fig. 7Ci**). Tau uptake was slightly decreased in *LRP1* knockdown cells, which was subsequently quantified as a 30% reduction by flow cytometry (**Fig. 7Cii**). *LRP1*-siRNA3 knockdown exacerbated *IL-6* gene expression increases as compared to negative control cells in response to tau (**Fig. 7D**), suggesting an intermediate regulatory role of LRP1 in response to inflammatory stimuli. Interestingly, ERK appeared unresponsive in *LRP1* knockdown cells (**Fig. 7E**), implying that other possible as yet unknown signaling pathways, regulated by LRP1, may be also responsible for the activation of immune pathways following tau uptake.

Discussion

Rapid HSPG-dependent endocytosis of tau monomers

Extracellular tau is present in brain cerebrospinal fluid (CSF) and interstitial fluid (ISF) of AD patients either as free tau or within vesicles [16]. The majority of extracellular tau consists of soluble oligomers and monomers, while a minority of tau species are in a truncated form from cleavage by various pro-inflammatory cytokines released by reactive astrocytes and microglia in AD brains [60]. The cellular internalization of extracellular tau is a major part of neurodegenerative disease progression, which is still under investigation [61]. The cellular pathways of tau internalization are highly dependent on the overall size of tau species, ranging from receptor-mediated endocytosis to actin-dependent macropinocytosis [25][45]. Importantly, HSPGs, highly expressed on the cell surface, have been identified as an important cell-surface endocytosis receptor of tau in various studies [45][62]. Ranch and coworkers reported that knockouts of extension enzymes of the HSPG biosynthetic pathway, such as extension enzymes exostosin 1 (EXT1), exostosin 2 (EXT2), and exostosin-like 3 (EXTL3) sufficiently reduced the uptake of tau oligomers in HEK293 cells [26]. Primary neurons and mouse models with heparin pretreatment showed diminished tau aggregate uptake, suggesting HSPGs are required for tau aggregate internalization *in vivo* [45]. We have observed a similar effect of HSPGs on regulating, in particular, monomeric tau protein, using a more CNS relevant cell line. In our study, reduced tau uptake was observed in both CHO745 and *Xylt*-knockout C6 glial cell lines and indicated the role of HSPGs in tau uptake.

The interaction between tau monomers and HSPGs has also been characterized at the structural level characterized by surface plasmon resonance and NMR mapping. Several studies suggest that tau-

HSPG interactions are regulated by specific sulfation patterns of the HS chain, including 6-O-sulfation [26], 3-O-sulfation [63], and N-sulfation [64]. Interestingly, tau also contains a heparin-binding domain; residues in both the proline-rich region (PRR) and the second repeat motif (R2) have been shown to be specifically recognized by negatively charged sulfo groups on HS [63]. This suggests a complex regulation of tau interactions with HSPG and heparin that merit more attention in further studies.

Cellular events regulated by cell surface heparan sulfate proteoglycans

Cell surface HSPGs have been implicated in a variety of receptor signaling pathways via the binding of extracellular molecules and entities such as viruses [62]. HSPGs act as internalizing receptors of macromolecular cargo such as FGF2, lipoproteins, and ApoE in a receptor-independent mechanism via the clathrin-coated pit endocytosis pathway. There are two major classes of cell surface HSPGs, which are characterized by the type of core protein – the glypican (GPCs) family of glycosylphosphatidylinositol (GPI)-linked proteins and the syndecan family of transmembrane proteins [57]. Most relevant to our study, the binding of ligands to cell surface syndecan HSPG activates ERK1/2 signaling to facilitate actin-dependent endocytosis [62].

As a co-receptor, HSPGs activates receptor signaling following binding between cytokines and their corresponding receptors, such as the binding between FGF and FGFR and IL-6 and IL-6R [57]. For instance, a recent study demonstrated the inflammatory effects of low molecular weight heparin to attenuate IL-6 release in patients with COVID-19 by competing with HSPGs for the binding of IL-6 [65]. Moreover, the transcriptional level of *IL-6* was significantly decreased after the addition of a heparinase enzyme inhibitor. The underlying mechanism behind these effects was that cell surface HSPGs regulate IL-6 ligand-receptor interaction and IL-6 secretion via facilitating the activation of JAK associated with the IL-6 receptor. Downstream ERK 1/2 signaling has also been found to mediate the transcriptional activation of IL-6 [66]. An ERK1/2 inhibitor reduced the transcriptional level of *IL-6*, suggesting the ERK activation plays a role in transcription and subsequent IL-6 secretion. Here, no ERK1/2 signaling activation was observed in HSPG-deficient cells. Taken together, these data suggest that HSPG interactions play a critical role in regulating inflammatory gene expression in glial cells following the addition of exogenous monomeric tau via intracellular ERK1/2 signaling activation (**Fig. 8**). However, further study is needed to identify the primary contributor to ERK1/2 phosphorylation, HSPG-dependent endocytosis of tau or positive-feedback regulation of IL-6 secretion, or both.

Differential Tau-HSPG interaction defined by specific tau variants

Previous work describes a 'paperclip-like' conformation for tau in solution, where the N- and C-terminal ends fold over in proximity to the center of the repeat domains [67]. Site-specific phosphorylation and mutations have been found to directly impact the conformation of monomeric tau and affect the stability of a folded conformation, contributing to the propensity for tau protein to aggregate [68]. A recent study reported that FTD-associated mutations enhanced tau oligomer internalization in SH-SY5Y cells, presenting *in vitro* evidence that mutation-induced conformational changes may lead to changes in tau binding to HSPGs on the cell surface [69]. Indeed, site-specific modifications of tau monomer may cause conformational changes to tau structure that facilitate conversion of inert wild-type tau into seed-competent tau states that have a high propensity to form aggregates and filaments [18]. In our study, no significant difference was observed in monomeric tau uptake between different protein variants within 30 minutes. Nevertheless, differential pro-inflammatory gene expression and ERK1/2 phosphorylation was observed with these variants. This result implies that differential tau-HSPG interaction may be responsible for intracellular change; further investigation of tau protein variant binding to heparan sulfate proteoglycans may uncover differential affinities. Alternatively, changes to the tau variants following uptake – such as aggregation or phosphorylation – could alter intracellular pathways. To our knowledge, our study is the first that finds different tau variants' behavior in activating downstream cellular pathways in a CNS-relevant cellular system, which argues that the tau-HSPG interaction may be also epitope and tau variant-dependent.

Crosstalk between LRP1 and HSPGs in regulating intracellular responses of glial cells to tau monomer

Apart from HSPG-dependent endocytosis, tau internalization is also regulated by specific receptor-mediated endocytosis, as suggested by several previous reports [25][58]. LRP1 has recently been recognized as a master regulator of tau uptake; *LRP1* knockdown abolished uptake of various forms of tau including monomers, oligomers, and fibrils in H4 neuroglioma cells [58]. Our study showed consistent results as observed in neuronal cells, demonstrating the involvement of LRP1 in tau endocytosis by glial cells. In addition, the cooperative interplay between HSPGs and LRP1 has been found to regulate neuronal Aβ uptake [70]. Interestingly, LRP1 has been shown to facilitate the endocytosis and lysosomal degradation of the HSPG-hedgehog complex [71], suggesting a possible LRP1-based regulation of HSPG-dependent endocytosis.

In our study, downregulation of *LRP1* mRNA was observed in the glial cells upon monomeric tau addition, while *LRP1* remained at a similar level in HSPG-deficient cells compared to control cells upon tau addition. Further, *LRP1* knockdown exaggerated *IL-6* mRNA expression, while no ERK activation was

observed. Thus, we suggest that IL-6 changes likely were altered via the JNK pathway (**Fig. 8**). Alternatively, upregulated *IL-6* expression may be the outcome of cooperation between LRP1 and HSPG via its binding to monomeric tau. Further studies are needed to identify the intracellular signaling pathways involved in the immune response of glial cells to tau, with a special focus on the MAPK and JNK pathways, which have been previously identified as the key protein kinases regulated by Aβ-LRP1 interaction in microglial cells [59].

Implications of efficient monomeric tau endocytosis for tau pathogenesis

Extensive studies suggest that the progression of tau pathologies including FTD, Pick disease, progressive supranuclear palsy and corticobasal degeneration, rely on the effective spreading of pathogenic tau, known as 'seeds', along both synaptic and non-synaptic pathways [61][72]. This propagation of tau pathology involves the transfer of pathogenic tau seeds from 'recipient cell' to 'donor cell' and templated-seeding of aggregation via recruitment of normal tau and formation of new tau seeds in donor cells [73]. Several studies have shown that soluble tau oligomers may act as the toxic seeds inducing endogenous tau misfolding [74] and transneuronal propagation [15]. However, monomeric tau internalization has been less well investigated as it has been considered less pathogenic. Given the abundance of monomeric tau in neurons, as well as the presence of extracellular tau in the ISF and CSF, monomeric tau may serve a role in the pathogenesis of tauopathies under as yet unknown conditions. Even though the templating-seeding properties of tau seeds mostly rely on the recruitment of endogenous tau protein [61], rapid endocytosis of monomeric tau protein has provided higher levels of intracellular tau protein available for seeding in both neuronal cells and astrocytes. It remains more plausible that this seeding occurs under pathological conditions where tau seeds facilitate intracellular tau aggregate formation [30][75]. Phosphorylated tau protein may have a higher seeding propensity since phosphorylated tau was more sensitive to heparin-induced aggregation compared to wild-type protein based on *in vitro* study [76].

Our results show more abundant and rapid accumulation of tau protein in astrocytic-like cells compared to neuronal cells, which is consistent with prior work demonstrating astrocytes exhibit greater avidity for oligomeric tau than neurons [77]. Astrocytes are enriched in phagocytosis pathways, suggesting the natural cellular mechanisms of enhanced uptake increased tau internalization by astrocytes as compared to neurons. For instance, astrogliosis has been observed concurrent with the upregulation of TFEB (transcriptional factor EB) – a key regulator of phagocytosis in astrocytes – within a range of clinical neurodegenerative diseases [78]. Astrocytic internalization of tau disrupted intracellular Ca^{2+} signaling, leading to a significant reduction in the levels of released gliotransmitters and synaptic vesicles, in an ATP-dependent manner [77]. Informed by these previous studies, rapid endocytosis of monomeric tau by

astrocytes observed in our study would likely alter astrocytic neurotransmission, causing synaptic degeneration. We suggest that the seeding propensity for aggregation and potential alterations in neurotransmission following uptake of monomeric tau may have an overlapping role in the progression of tau pathogenesis. Future studies will focus on further investigating the functional alterations in CNS cell lines following monomeric tau internalization.

Conclusions

Our study shows that monomeric tau is rapidly endocytosed by multiple CNS-relevant cell lines, and the fastest tau endocytosis rate was observed in glial cells among all the cell types tested. In addition, we have demonstrated that tau endocytosis is facilitated by multiple pathways including actin-dependent macropinocytosis as well as HSPG- and LRP1-dependent pathways. Moreover, HSPG-mediated tau endocytosis in glial cells also triggered the downstream upregulation of pro-inflammatory gene expression, in part via mediating ERK1/2 signaling activation. Further, ERK1/2 phosphorylation also displayed a tau variant-dependent activation, where disease-relevant tau variants induced the highest levels of ERK1/2 phosphorylation. Further investigation also revealed the pivotal role of LRP1 in regulating the pro-inflammatory gene expression and tau internalization via altering the expression level of *LRP1*. The study has provided experimental evidence to advance the understanding of the important role of monomeric tau uptake in glial cells in the progression of tau pathology.

References

1. Lee VM-Y, Goedert M, Trojanowski JQ (2001) Neurodegenerative Tauopathies. Annu Rev Neurosci 24:1121–1159. https://doi.org/10.1146/annurev.neuro.24.1.1121
2. Bramblett GT, Goedert M, Jakes R, et al (1993) Abnormal tau phosphorylation at Ser396 in alzheimer's disease recapitulates development and contributes to reduced microtubule binding. Neuron 10:1089–1099. https://doi.org/10.1016/0896-6273(93)90057-X
3. Zhang B, Higuchi M, Yoshiyama Y, et al (2004) Retarded axonal transport of R406W mutant tau in transgenic mice with a neurodegenerative tauopathy. J Neurosci 24:4657–4667. https://doi.org/10.1523/JNEUROSCI.0797-04.2004
4. Wang Y, Mandelkow E (2016) Tau in physiology and pathology. Nat. Rev. Neurosci.
5. Dujardin S, Bégard S, Caillierez R, et al (2014) Ectosomes: A new mechanism for non-exosomal secretion of Tau protein. PLoS One. https://doi.org/10.1371/journal.pone.0100760
6. Cummings J, Lee G, Ritter A, Zhong K (2018) Alzheimer's disease drug development pipeline: 2018. Alzheimer's Dement Transl Res Clin Interv 4:195–214. https://doi.org/10.1016/j.trci.2018.03.009
7. Barten DM, Cadelina GW, Hoque N, et al (2011) Tau transgenic mice as models for cerebrospinal fluid tau biomarkers. J Alzheimer's Dis 24:127–141. https://doi.org/10.3233/JAD-2011-110161
8. Wang Y, Balaji V, Kaniyappan S, et al (2017) The release and trans-synaptic transmission of Tau via exosomes. Mol Neurodegener 12:5. https://doi.org/10.1186/s13024-016-0143-y
9. Furman JL, Vaquer-Alicea J, White CL, et al (2017) Widespread tau seeding activity at early Braak stages. Acta Neuropathol 133:91–100. https://doi.org/10.1007/s00401-016-1644-z
10. Yamada K, Cirrito JR, Stewart FR, et al (2011) In vivo microdialysis reveals age-dependent decrease of brain interstitial fluid tau levels in P301S human tau transgenic mice. J Neurosci 31:13110–13117. https://doi.org/10.1523/JNEUROSCI.2569-11.2011
11. Sengupta U, Portelius E, Hansson O, et al (2017) Tau oligomers in cerebrospinal fluid in Alzheimer's disease. Ann Clin Transl Neurol 4:226–235. https://doi.org/10.1002/acn3.382
12. Saman S, Kim WH, Raya M, et al (2012) Exosome-associated tau is secreted in tauopathy models and is selectively phosphorylated in cerebrospinal fluid in early Alzheimer disease. J Biol Chem 287:3842–3849. https://doi.org/10.1074/jbc.M111.277061
13. Kanmert D, Cantlon A, Muratore CR, et al (2015) C-terminally truncated forms of tau, but not full-length tau or its C-terminal fragments, are released from neurons independently of cell death. J Neurosci 35:10851–10865. https://doi.org/10.1523/JNEUROSCI.0387-15.2015
14. Karch CM, Jeng AT, Goate AM (2012) Extracellular tau levels are influenced by variability in tau that is associated with tauopathies. J Biol Chem 287:42751–42762.

https://doi.org/10.1074/jbc.M112.380642
15. Pooler AM, Polydoro M, Wegmann S, et al (2013) Propagation of tau pathology in Alzheimer's disease: Identification of novel therapeutic targets. Alzheimer's Res. Ther. 5:49
16. Merezhko M, Brunello CA, Yan X, et al (2018) Secretion of Tau via an Unconventional Non-vesicular Mechanism. Cell Rep 25:. https://doi.org/10.1016/j.celrep.2018.10.078
17. Katsinelos T, Zeitler M, Dimou E, et al (2018) Unconventional Secretion Mediates the Trans-cellular Spreading of Tau. Cell Rep 23:2039–2055. https://doi.org/10.1016/j.celrep.2018.04.056
18. Mirbaha H, Chen D, Morazova OA, et al (2018) Inert and seed-competent tau monomers suggest structural origins of aggregation. Elife 7:. https://doi.org/10.7554/eLife.36584
19. Sharma AM, Thomas TL, Woodard DR, et al (2018) Tau monomer encodes strains. bioRxiv. https://doi.org/10.1101/325043
20. Michel CH, Kumar S, Pinotsi D, et al (2014) Extracellular monomeric tau protein is sufficient to initiate the spread of tau protein pathology. J Biol Chem. https://doi.org/10.1074/jbc.M113.515445
21. Takeda S, Wegmann S, Cho H, et al (2015) Neuronal uptake and propagation of a rare phosphorylated high-molecular-weight tau derived from Alzheimer's disease brain. Nat Commun 6:1–15. https://doi.org/10.1038/ncomms9490
22. Mirbaha H, Holmes BB, Sanders DW, et al (2015) Tau trimers are the minimal propagation unit spontaneously internalized to seed intracellular aggregation. J Biol Chem 290:14893–14903. https://doi.org/10.1074/jbc.M115.652693
23. Frost B, Jacks RL, Diamond MI (2009) Propagation of Tau misfolding from the outside to the inside of a cell. J Biol Chem 284:12845–12852. https://doi.org/10.1074/jbc.M808759200
24. Wu JW, Herman M, Liu L, et al (2012) Small Misfolded Tau Species Are Internalized via Bulk Endocytosis and Anterogradely and Retrogradely Transported in Neurons *. https://doi.org/10.1074/jbc.M112.394528
25. Evans LD, Wassmer T, Fraser G, et al (2018) Extracellular Monomeric and Aggregated Tau Efficiently Enter Human Neurons through Overlapping but Distinct Pathways. Cell Rep 22:3612–3624. https://doi.org/10.1016/j.celrep.2018.03.021
26. Rauch JN, Chen JJ, Sorum AW, et al (2018) Tau Internalization is Regulated by 6-O Sulfation on Heparan Sulfate Proteoglycans (HSPGs). Sci Rep 8:. https://doi.org/10.1038/s41598-018-24904-z
27. Elbaum-Garfinkle S, Rhoades E (2012) Identification of an aggregation-prone structure of tau. J Am Chem Soc 134:16607–16613. https://doi.org/10.1021/ja305206m
28. Song L, Wells EA, Robinson AS (2021) Critical Molecular and Cellular Contributors to Tau Pathology. Biomedicines 9:190. https://doi.org/10.3390/biomedicines9020190
29. Sidoryk-Wegrzynowicz M, Gerber YN, Ries M, et al (2017) Astrocytes in mouse models of

tauopathies acquire early deficits and lose neurosupportive functions. Acta Neuropathol Commun 5:89. https://doi.org/10.1186/s40478-017-0478-9

30. Leyns CEG, Holtzman DM (2017) Glial contributions to neurodegeneration in tauopathies. Mol. Neurodegener. 12:1–16
31. Cahoy JD, Emery B, Kaushal A, et al (2008) A transcriptome database for astrocytes, neurons, and oligodendrocytes: A new resource for understanding brain development and function. J Neurosci 28:264–278. https://doi.org/10.1523/JNEUROSCI.4178-07.2008
32. Kim Y, Park J, Choi YK (2019) The role of astrocytes in the central nervous system focused on BK channel and heme oxygenase metabolites: A review. Antioxidants 8:121. https://doi.org/10.3390/antiox8050121
33. Li Y, Cheng D, Cheng R, et al (2014) Mechanisms of U87 Astrocytoma Cell Uptake and Trafficking of Monomeric versus Protofibril Alzheimer's Disease Amyloid-β Proteins. PLoS One 9:e99939. https://doi.org/10.1371/journal.pone.0099939
34. Liddelow SA, Guttenplan KA, Clarke LE, et al (2017) Neurotoxic reactive astrocytes are induced by activated microglia. Nature 541:481–487. https://doi.org/10.1038/nature21029
35. Morozova O a, March ZM, Robinson AS, Colby DW (2013) Conformational Features of Tau Fibrils from Alzheimer ' s Disease Brain Are Faithfully Propagated by Unmodi fi ed Recombinant Protein
36. Flanagan LA, Cunningham CC, Chen J, et al (1997) The structure of divalent cation-induced aggregates of PIP2 and their alteration by gelsolin and tau. Biophys J. https://doi.org/10.1016/S0006-3495(97)78176-1
37. Gómez-Ramos A, Díaz-Hernández M, Rubio A, et al (2008) Extracellular tau promotes intracellular calcium increase through M1 and M3 muscarinic receptors in neuronal cells. Mol Cell Neurosci. https://doi.org/10.1016/j.mcn.2007.12.010
38. Gómez-Ramos A, Díaz-Hernández M, Rubio A, et al (2009) Characteristics and consequences of muscarinic receptor activation by tau protein. Eur Neuropsychopharmacol. https://doi.org/10.1016/j.euroneuro.2009.04.006
39. Yang Z, Steentoft C, Hauge C, et al (2015) Fast and sensitive detection of indels induced by precise gene targeting. Nucleic Acids Res 43:e59–e59. https://doi.org/10.1093/nar/gkv126
40. Bejoy J, Bijonowski B, Marzano M, et al (2020) Wnt-notch signaling interactions during neural and astroglial patterning of human stem cells. Tissue Eng - Part A 26:419–431. https://doi.org/10.1089/ten.tea.2019.0202
41. Song L, Yuan X, Jones Z, et al (2019) Functionalization of Brain Region-specific Spheroids with Isogenic Microglia-like Cells. Sci Rep 9:1–18. https://doi.org/10.1038/s41598-019-47444-6

42. Agholme L, Lindström T, Kgedal K, et al (2010) An in vitro model for neuroscience: Differentiation of SH-SY5Y cells into cells with morphological and biochemical characteristics of mature neurons. J Alzheimer's Dis 20:1069–1082. https://doi.org/10.3233/JAD-2010-091363
43. Ghoshal N, García-Sierra F, Fu Y, et al (2001) Tau-66: evidence for a novel tau conformation in Alzheimer's disease. J Neurochem 77:1372–1385. https://doi.org/10.1046/j.1471-4159.2001.00346.x
44. Ferrer I, López-González I, Carmona M, et al (2014) Glial and neuronal tau pathology in tauopathies: Characterization of disease-specific phenotypes and tau pathology progression. J Neuropathol Exp Neurol. https://doi.org/10.1097/NEN.0000000000000030
45. Holmes BB, DeVos SL, Kfoury N, et al (2013) Heparan sulfate proteoglycans mediate internalization and propagation of specific proteopathic seeds. Proc Natl Acad Sci U S A 110:E3138–E3147. https://doi.org/10.1073/pnas.1301440110
46. Murakami S, Takenaka-Uema A, Kobayashi T, et al (2017) Heparan Sulfate Proteoglycan Is an Important Attachment Factor for Cell Entry of Akabane and Schmallenberg Viruses. J Virol. https://doi.org/10.1128/jvi.00503-17
47. Lidholt K, Weinke JL, Kiser CS, et al (1992) A single mutation affects both N-acetylglucosaminyltransferase and glucuronosyltransferase activities in a Chinese hamster ovary cell mutant defective in heparan sulfate biosynthesis. Proc Natl Acad Sci U S A 89:2267–2271. https://doi.org/10.1073/pnas.89.6.2267
48. Cong L, Zhang F (2014) Genome engineering using crispr-cas9 system. In: Chromosomal Mutagenesis: Second Edition. pp 197–217
49. Stancu IC, Cremers N, Vanrusselt H, et al (2019) Aggregated Tau activates NLRP3–ASC inflammasome exacerbating exogenously seeded and non-exogenously seeded Tau pathology in vivo. Acta Neuropathol 137:599–617. https://doi.org/10.1007/s00401-018-01957-y
50. Swanson K V., Deng M, Ting JPY (2019) The NLRP3 inflammasome: molecular activation and regulation to therapeutics. Nat. Rev. Immunol. 19:477–489
51. Ferrer I, Blanco R, Carmona M, et al (2001) Phosphorylated map kinase (ERK1, ERK2) expression is associated with early tau deposition in neurones and glial cells, but not with increased nuclear DNA vulnerability and cell death, in Alzheimer disease, Pick's disease, progressive supranuclear palsy an. Brain Pathol 11:144–158. https://doi.org/10.1111/j.1750-3639.2001.tb00387.x
52. Pei JJ, Braak H, An WL, et al (2002) Up-regulation of mitogen-activated protein kinases ERK1/2 and MEK1/2 is associated with the progression of neurofibrillary degeneration in Alzheimer's disease. Mol Brain Res 109:45–55. https://doi.org/10.1016/S0169-328X(02)00488-6

53. Chua CC, Rahimi N, Forsten-Williams K, Nugent MA (2004) Heparan Sulfate Proteoglycans Function as Receptors for Fibroblast Growth Factor-2 Activation of Extracellular Signal-Regulated Kinases 1 and 2. Circ Res 94:316–323. https://doi.org/10.1161/01.RES.0000112965.70691.AC
54. Tanemura K, Murayama M, Akagi T, et al (2002) Neurodegeneration with tau accumulation in a transgenic mouse expressing V337M human tau. J Neurosci 22:133–141. https://doi.org/10.1523/jneurosci.22-01-00133.2002
55. Vogelsberg-Ragaglia V, Bruce J, Richter-Landsberg C, et al (2000) Distinct FTDP-17 missense mutations in tau produce tau aggregates and other pathological phenotypes in transfected CHO cells. Mol Biol Cell 11:4093–4104. https://doi.org/10.1091/mbc.11.12.4093
56. Lim S, Haque MM, Kim D, et al (2014) Cell-based models to investigate Tau aggregation. Comput. Struct. Biotechnol. J. 12:7–13
57. Lin X (2004) Functions of heparan sulfate proteoglycans in cell signaling during development. Development 131:6009–6021
58. Rauch JN, Luna G, Guzman E, et al (2020) LRP1 is a master regulator of tau uptake and spread. Nature 580:381–385. https://doi.org/10.1038/s41586-020-2156-5
59. Yang L, Liu CC, Zheng H, et al (2016) LRP1 modulates the microglial immune response via regulation of JNK and NF-KB signaling pathways. J Neuroinflammation 13:. https://doi.org/10.1186/s12974-016-0772-7
60. Dal Prà I, Chiarini A, Gui L, et al (2015) Do astrocytes collaborate with neurons in spreading the "infectious" aβ and Tau drivers of Alzheimer's disease? Neuroscientist 21:9–29. https://doi.org/10.1177/1073858414529828
61. Holmes BB, Diamond MI (2014) Prion-like properties of Tau protein: The importance of extracellular Tau as a therapeutic target. J. Biol. Chem. 289:19855–19861
62. Christianson HC, Belting M (2014) Heparan sulfate proteoglycan as a cell-surface endocytosis receptor. Matrix Biol 35:51–55. https://doi.org/10.1016/j.matbio.2013.10.004
63. Zhao J, Zhu Y, Song X, et al (2020) 3- *O* -Sulfation of Heparan Sulfate Enhances Tau Interaction and Cellular Uptake. Angew Chemie Int Ed 59:1818–1827. https://doi.org/10.1002/anie.201913029
64. Barbara Stopschinski XE, Holmes BB, Miller GM, et al (2018) Specific glycosaminoglycan chain length and sulfation patterns are required for cell uptake of tau versus-synuclein and-amyloid aggregates. https://doi.org/10.1074/jbc.RA117.000378
65. Shi C, Wang C, Wang H, et al (2020) The Potential of Low Molecular Weight Heparin to Mitigate Cytokine Storm in Severe COVID-19 Patients: A Retrospective Cohort Study. Clin Transl Sci 13:.

https://doi.org/10.1111/cts.12880

66. Maddahi A, Povlsen G, Edvinsson L (2012) Regulation of enhanced cerebrovascular expression of proinflammatory mediators in experimental subarachnoid hemorrhage via the mitogen-activated protein kinase kinase/extracellular signal-regulated kinase pathway. J Neuroinflammation 9:783. https://doi.org/10.1186/1742-2094-9-274
67. Jeganathan S, Von Bergen M, Brutlach H, et al (2006) Global hairpin folding of tau in solution. Biochemistry 45:2283–2293. https://doi.org/10.1021/bi0521543
68. Tenreiro S, Eckermann K, Outeiro TF (2014) Protein phosphorylation in neurodegeneration: Friend or foe? Front. Mol. Neurosci. 7
69. Karikari TK, Nagel DA, Grainger A, et al (2019) Distinct Conformations, Aggregation and Cellular Internalization of Different Tau Strains. Front Cell Neurosci 13:296. https://doi.org/10.3389/fncel.2019.00296
70. Kanekiyo T, Zhang J, Liu Q, et al (2011) Heparan sulphate proteoglycan and the low-density lipoprotein receptor-related protein 1 constitute major pathways for neuronal amyloid-β uptake. J Neurosci 31:1644–1651. https://doi.org/10.1523/JNEUROSCI.5491-10.2011
71. Capurro MI, Shi W, Filmus J (2012) LRP1 mediates Hedgehog-induced endocytosis of the GPC3-Hedgehog complex. J Cell Sci 125:3380–3389. https://doi.org/10.1242/jcs.098889
72. Hock E-M, Polymenidou M (2016) Prion-like propagation as a pathogenic principle in frontotemporal dementia. J Neurochem 138:163–183. https://doi.org/10.1111/jnc.13668
73. Mudher A, Colin M, Dujardin S, et al (2017) What is the evidence that tau pathology spreads through prion-like propagation? Acta Neuropathol. Commun. 5:99
74. Shafiei SS, Guerrero-Muñoz MJ, Castillo-Carranza DL (2017) Tau oligomers: Cytotoxicity, propagation, and mitochondrial damage. Front. Aging Neurosci. 9
75. Guo JL, Lee VMY (2011) Seeding of normal tau by pathological tau conformers drives pathogenesis of Alzheimer-like tangles. J Biol Chem 286:15317–15331. https://doi.org/10.1074/jbc.M110.209296
76. Alonso ADC, Zaidi T, Novak M, et al (2001) Hyperphosphorylation induces self-assembly of τ into tangles of paired helical filaments/straight filaments. Proc Natl Acad Sci U S A 98:6923–6928. https://doi.org/10.1073/pnas.121119298
77. Piacentini R, Li Puma DD, Mainardi M, et al (2017) Reduced gliotransmitter release from astrocytes mediates tau-induced synaptic dysfunction in cultured hippocampal neurons. Glia 65:1302–1316. https://doi.org/10.1002/glia.23163

78. Martini-Stoica H, Cole AL, Swartzlander DB, et al (2018) TFEB enhances astroglial uptake of extracellular tau species and reduces tau spreading. J Exp Med 215:2355–2377. https://doi.org/10.1084/jem.20172158

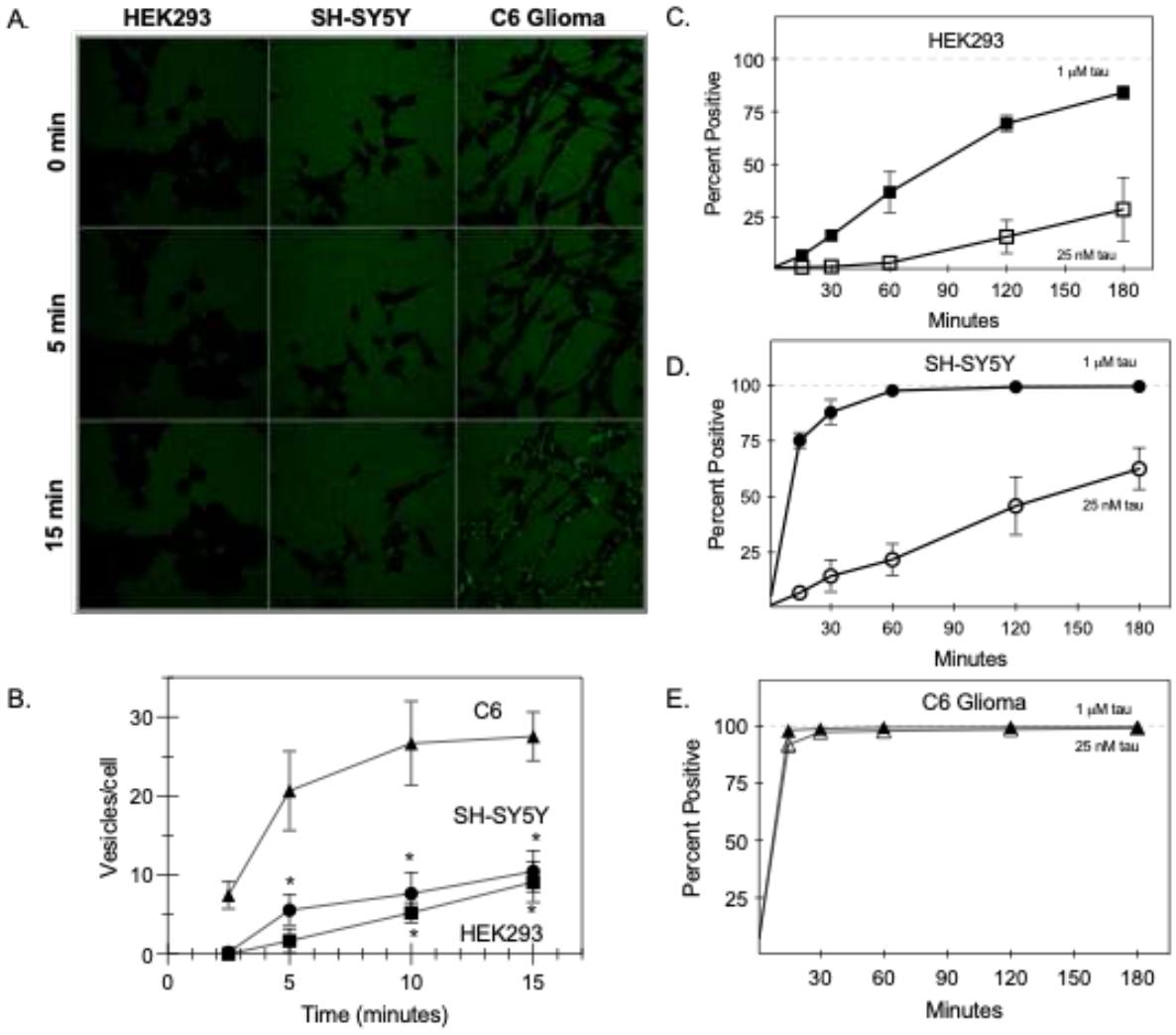

Fig.1 Cell type differences in tau uptake. A. Representative confocal microscopy images for HEK293, SH-SY5Y, and C6 glioma following addition of 1 μM 0N4R tau monomer. Scale bar = 10 μM. **B.** Quantification of live-cell confocal microscopy: C6 glioma cells (triangles) endocytose 0N4R monomer about three to four times faster compared to SH-SY5Y cells (circles) and HEK293 cells (squares) (* represents $p<0.05$ between C6 and the other two cell types) **C-E.** Flow cytometry data. For HEK293 cells (C) reducing the concentration of tau-488 to 25 nM (open squares) significantly reduced the tau internalization. For SH-SY5Y cells (D), the internalization was reduced at 25 nM (open circles), while for C6 glioma cells (E), there was no observed difference between the concentrations.

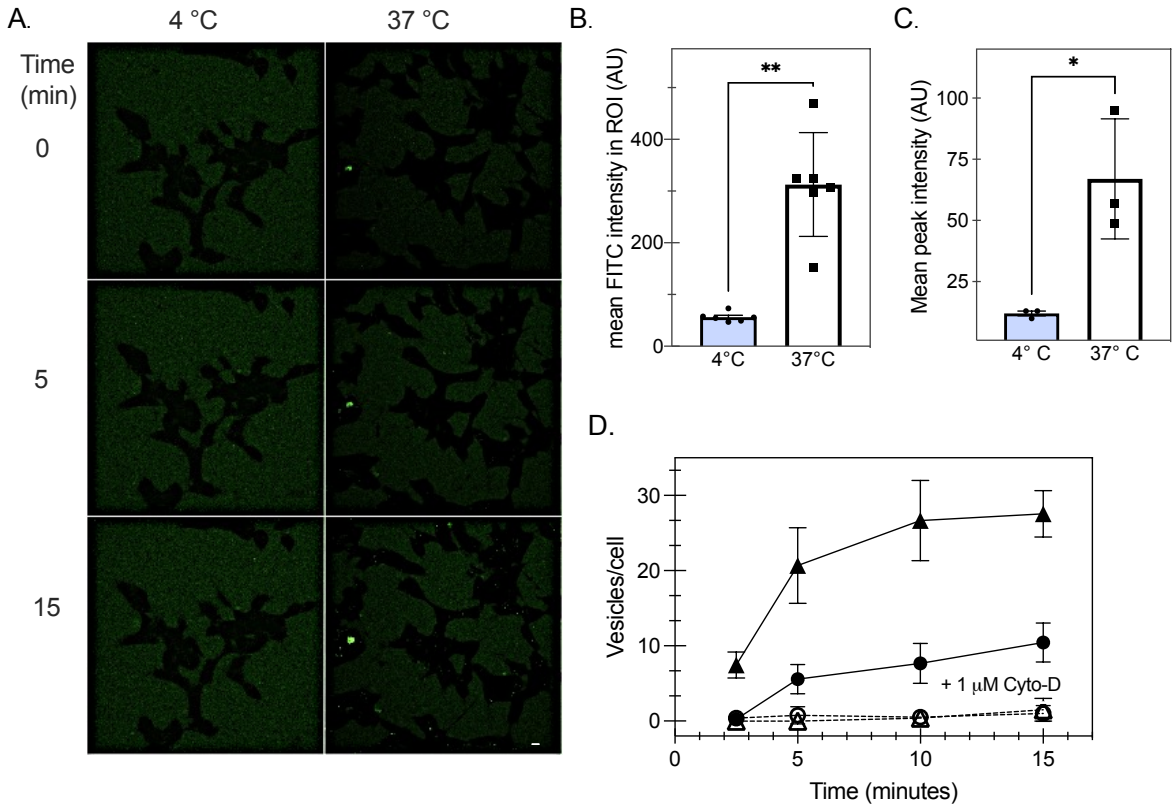

Fig. 2 Monomeric tau is internalized via actin-mediated endocytosis. A. Representative confocal microscopy images of HEK293 cells incubated with 1 μM tau-488. Scale bar = 10 μM. **B.** Pre-incubating HEK293 cells on wet ice (4 °C) prevents tau uptake as measured by confocal microscopy analysis of mean fluorescence intensity (** represents $p<0.005$, unpaired t-test of 37°C compared with 4°C, n>10/image). Individual points represent individual cells where bars show mean and SEM. **C.** Pre-incubating HEK293 cells on wet ice (4 °C) decreases tau uptake compared with cells at 37 °C as measured by mean peak intensity via flow cytometry (* represents $p<0.05$ for the 37°C compared to 4°C; n=3 independent replicates). Individual points represent individual cells where bars show mean and SEM. **D.** 1 μM cytochalasin-D (open symbols, cyto-D) decreases the rate of tau-488 internalization in SH-SY5Y (circles) and C6 glioma cells (triangles) compared with untreated cells (filled symbols; $p<0.05$ for 1 μM compared to untreated cells) observed by confocal microscopy.

A.

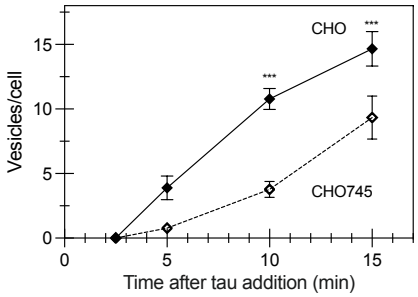

B.

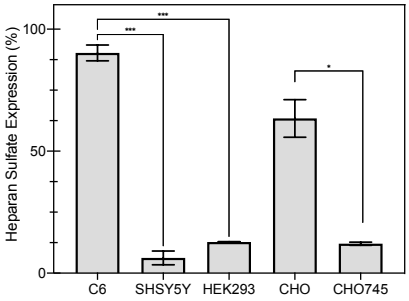

Fig. 3 Tau monomer uptake depends on HSPG levels. A. When characterized by the number of vesicles per cell observed via live-cell imaging, CHO745 cells had significantly fewer tau-containing vesicles per cell compared with wild-type CHO cells (* represents $p<0.05$ for CHO745 cells compared with wild-type cells; n=9, where points are the average, and error bars represent the standard error). **B.** Heparan sulfate detection on the cell surface was determined via immunolabeling with anti-heparan sulfate antibodies and detected by flow cytometry, as described in materials and methods. (Bars represent the mean for n=2 , and error bars represent the standard error; * represents $p<0.05$ based on t-test; *** represents $p<0.001$ based on one-way ANOVA)

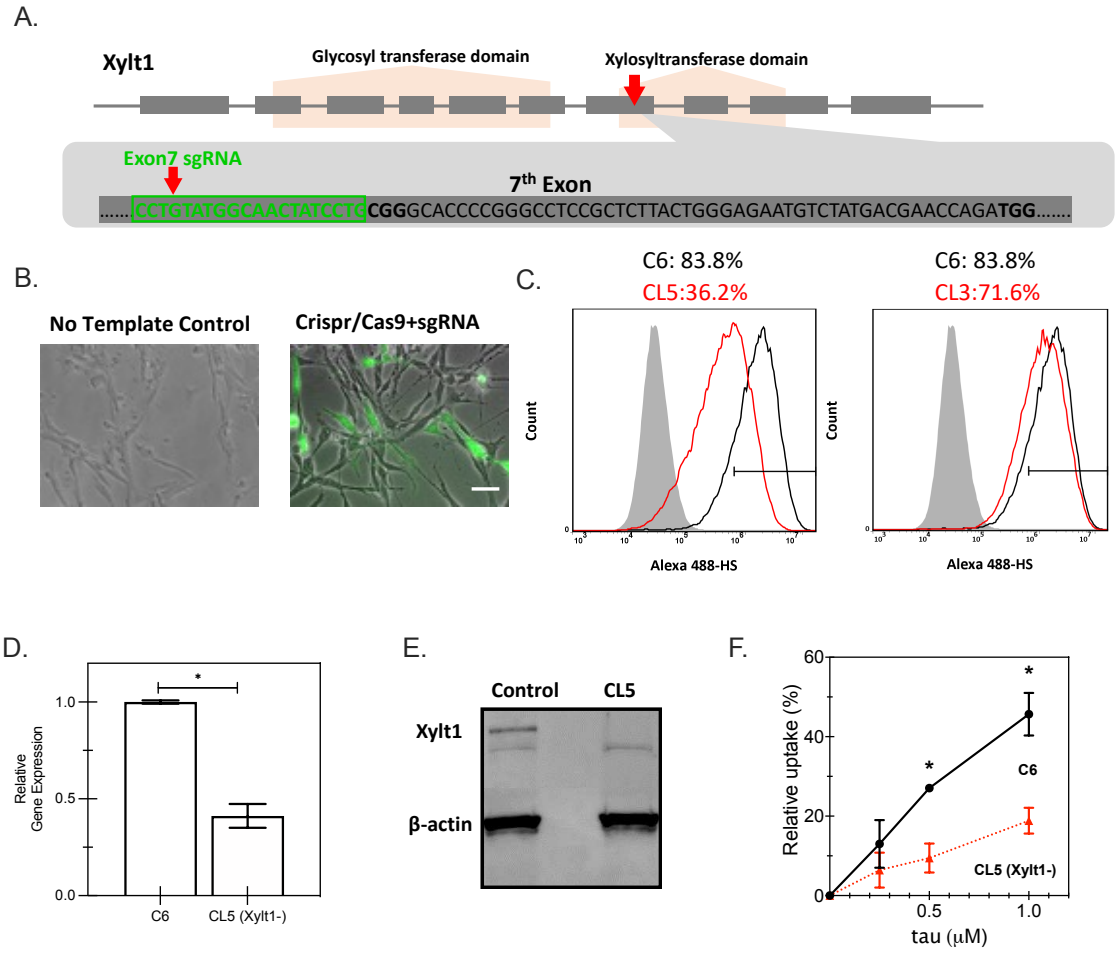

Fig. 4 Construction of a Xylt1 knockdown C6 glioma cell line with CRISPR/Cas9 genome editing technology. A. Schematic illustration of Xylt1 gene of *Rattus norvegicus*, containing two functional domains and 10 exons. Single guide RNA (sgRNA) was designed to target Exon7 of Xylt1 within the xylosyltransferase domain as indicated by the red arrow. The sgRNA sequence is highlighted in green. **B.** Overlay of phase-contrast images with fluorescent images of transfected C6 cells with either the control or the pre-constructed CRISPR/Cas9+sgRNA plasmid as indicated. Scale bar = 100 μm **C.** Quantification of Heparan sulfate (HS) expression by flow cytometry of non-edited C6 (C6), clone 5 (CL5), or clone 3 (CL3), showing highest knockdown for CL5. Shaded histogram: negative control; Black curve: parental C6 cells; Red curve: either C6 single-cell clone (CL) 5 or 3, as indicated. Xylt1 gene knockdown in clone 5 (CL5) was verified by both quantitative reverse transcription-polymerase reaction (RT-qPCR) **(D)**, where * indicates $p<0.05$ between different test conditions, and western blot analysis using Xylt1 antibody **(E). F.** The relative uptake of tau in C6 parental cells (filled circles) compared with CL5 cells (filled trianges) was quantified by flow cytometry after a thirty-minute incubation at the indicated concentrations. Error bars reflect the standard error, where * represents $p<0.05$ for CL5 cells compared with parental (n=2).

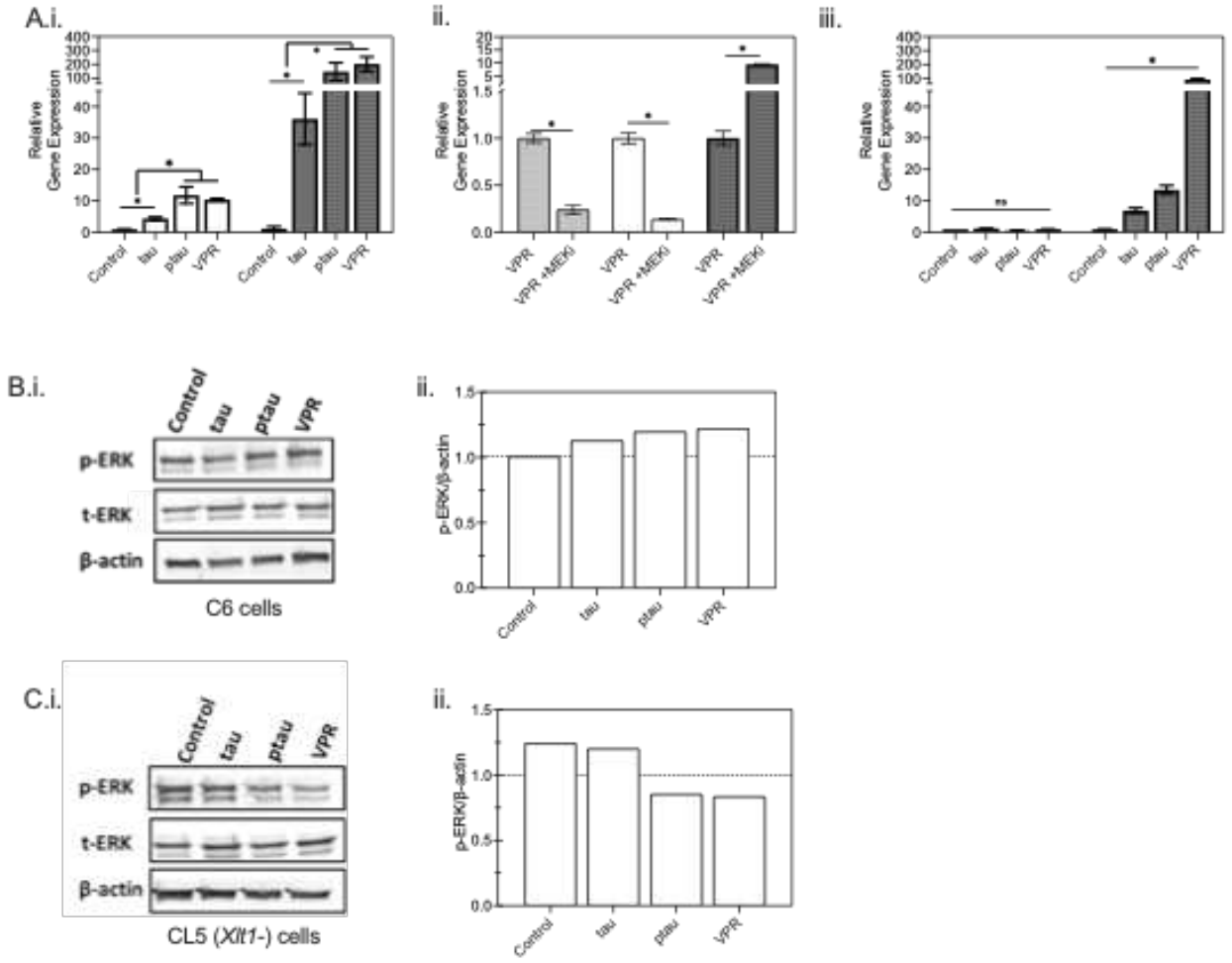

Fig.5 The role of HSPGs in regulating the immune response of glial cells to tau endocytosis is mediated by intracellular ERK1/2 signaling. A.C6 cells (**i** and **ii**) and and HSPG-deficient (*Xlt1*-) CL5 cells (**iii**), were incubated with different tau variants for 24 hrs. RNA was isolated and then subjected to quantitative reverse transcription-polymerase reaction (RT-qPCR) for relative mRNA expression quantification of IL-6 (open bars) and TNF-α (darkly shaded bars). In A.i., C6 cells were incubated with 1 μM VPR-0N4R along with MEK-ERK1/2 inhibitor or vehicle for 24 hrs. RNA was extracted and the relative mRNA levels of IL-1β (lightly shaded bars in **ii**), IL-6, and TNF-α were determined by RT-qPCR. * indicates $p<0.05$ between different test conditions; n=2. **B.** and **C.** Cell lysates were analyzed by western blotting for p-ERK1/2, total ERK (t-ERK), and β-actin in C6 (**B.i.**) and CL5 (**C.i.**). Quantification of p-ERK/β-actin ratios in C6 (**B.ii.**) and CL5 (**C.ii.**) from a representative western blot experiment are shown. Dashed line serves as a guide to the eye.

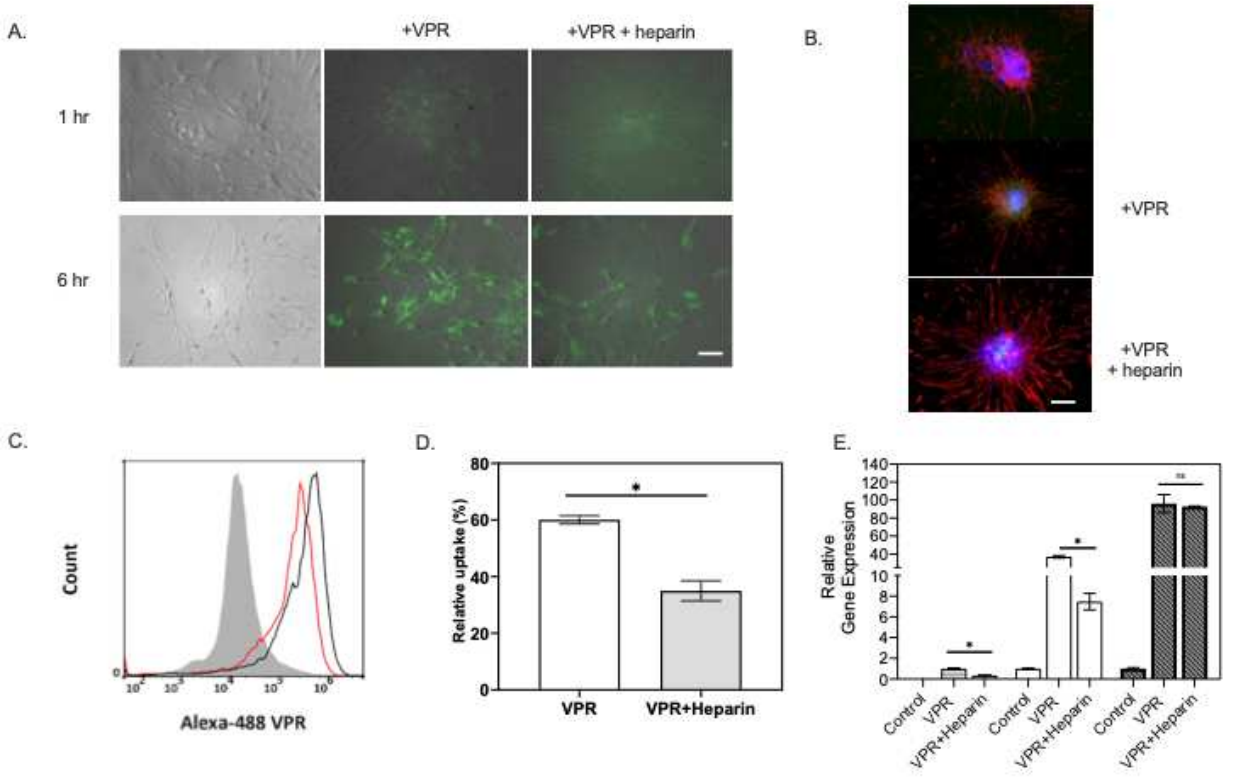

Fig.6 Rat primary astrocytes readily take up tau. A. The amount of VPR-0N4R labeled with AlexaFluor488 (+VPR, green) internalized by primary astrocytes increases over time from 1 hr to 6 hrs, while the presence of heparin has attenuated the tau uptake rate in astrocytes, as observed by fluorescence microscopy. Scale bar = 100 μm **B.** Representative fluorescent images of GFAP (red) and Hoechst (blue) for primary astrocytes under different conditions, as indicated, where VPR indicates the addition of VPR-488 with (middle panel) or without (bottom panel) heparin to the cell as observed via fluorescence microscopy. Scale bar = 100 μm **C.** To determine population behavior, VPR-488 endocytosed by primary astrocytes was determined by flow cytometry with and without heparin addition. Grey filled line: negative control; Black line: cells without heparin; red line: cells with heparin. **D.** The propensity of VPR-0N4R uptake was quantified in primary astrocytes by flow cytometry (n=2) **E.** An RT-qPCR analysis was performed to detect the expression levels of IL-1β (lightly shaded bars), IL-6 (open bars), and TNF-α (filled bars) in primary astrocytes affected by incubation with VPR and heparin, as indicated. β-Actin was used as an internal control. * indicates $p<0.05$ between different test conditions; n=2.

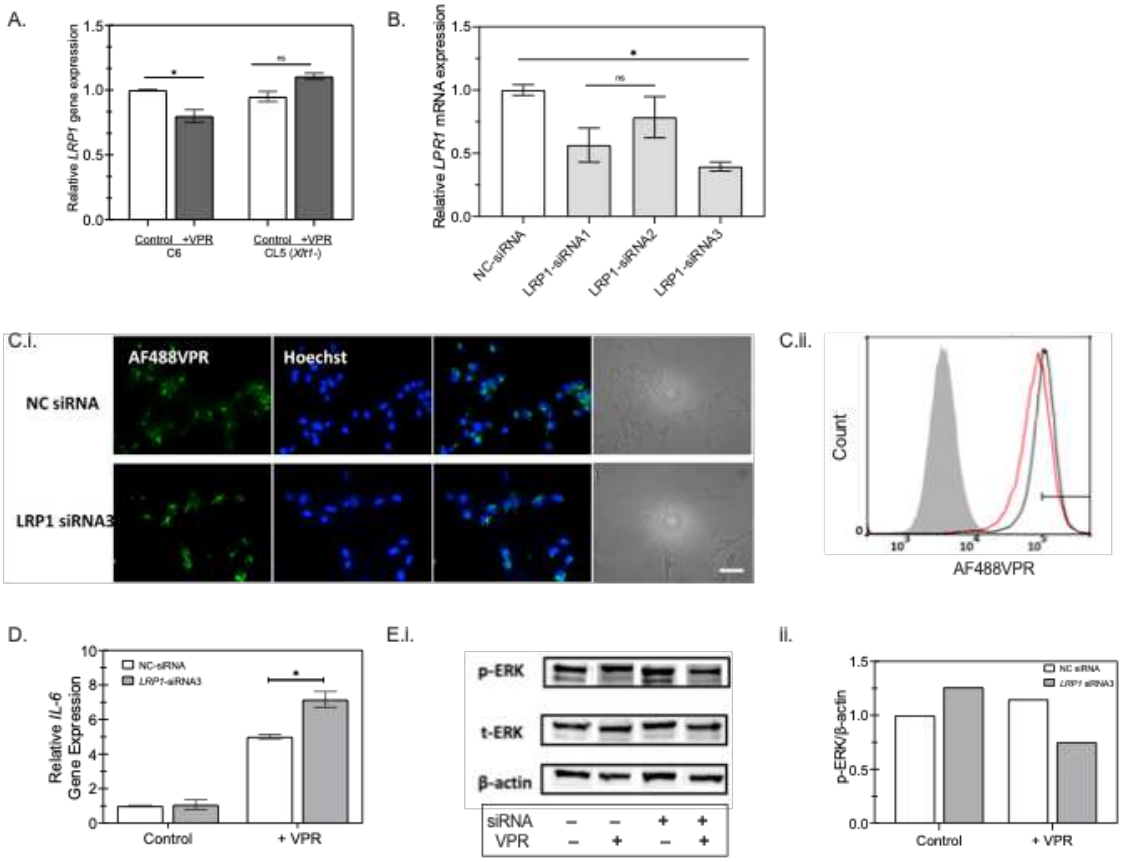

Fig.7 HSPGs are relevant to LRP-mediated tau endocytosis. A. Reduction of *LRP1* mRNA was observed for C6 cells but not for CL5 (*Xlt1*-) after incubation with 1 μM VPR (darkly shaded bars) for 24 hrs, as analyzed by RT-qPCR (n=2, * indicates $p<0.05$ between different conditions). **B.** Rat C6 glioma cells were transiently transfected with non-targeting siRNA (NC; open bars)) or *LRP1*-specific siRNA1, siRNA2, and siRNA3 for 48 hrs. *LRP1* knockdown was then confirmed by RT-PCR analysis. Darkly shaded bars indicate *LRP1*-specific siRNA, compared with NC-siRNA (open bars). (n=2, * indicates $p<0.05$ between different conditions). **C.i.** The propensity of AlexaFluor488-labeled monomeric VPR-0N4R (AF488VPR, green) uptake was examined in C6 cells post-transfection with non-targeting siRNA (NC) or *LRP1*-specific siRNA3 at 1 μM for 30 mins. Scale bar = 100 μm. **ii.** Flow cytometry histogram of AF488VPR uptake in NC siRNA cells (black curve) compared with *LRP1*-specific siRNA3 (red curve) shows quantitative decrease in tau uptake following knockdown. Gray filled curve shows distribution with vehicle only. Rat C6 glioma cells were transiently transfected with either non-targeting siRNA (NC) or *LRP1*-specific siRNA3 for 48, followed by incubation with 1 μM AF488VPR or vehicle for 24 hrs. **D.** RT-qPCR analysis was performed to detect the expression level of *IL-6* in C6 cells post-transfection as in (**C**), with β-Actin was used as an internal control. Open bars, NC-siRNA tranfected; Gray shaded bars, *LRP1*-siRNA3 (n=2, * indicates $p<0.05$ between different conditions) **E.** Cell lysates were then analyzed by immunoblotting (**i.**) against p-ERK1/2, total ERK (t-ERK), and β-actin, followed by quantitation (**ii.**) of p-

ERK/β-actin ratios from a representative western blot experiment. * indicates $p<0.05$ between different test conditions.

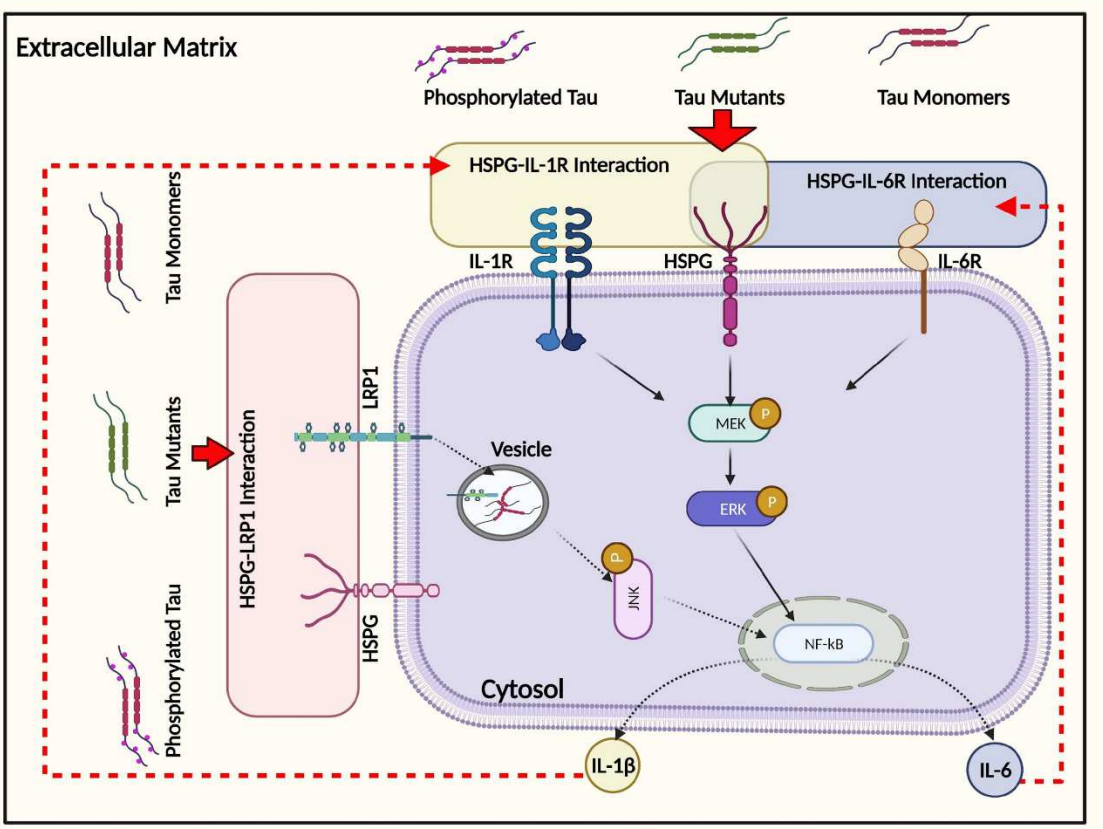

Fig. 8 Schematic illustration of the intracellular responses affected by monomeric tau endocytosis. Monomeric tau is rapidly internalized by both neuronal and glial cells, mediated by the actin-dependent macropinocytosis pathway. In addition, an important role of HSPG has been demonstrated in regulating inflammatory gene expression, including IL-6 and IL-1β, partially via ERK1/2 activation following tau uptake. LRP1 modulates IL-6 responses to tau endocytosis, and this interaction is HSPG-dependent but not ERK-dependent.

Supplementary Files

This is a list of supplementary files associated with this preprint. Click to download.

- SupplementaryMaterials.docx